

Short Blocklength Wiretap Channel Codes via Deep Learning: Design and Performance Evaluation

Vidhi Rana and Rémi A. Chou

Abstract

We design short blocklength codes for the Gaussian wiretap channel under information-theoretic security guarantees. Our approach consists in decoupling the reliability and secrecy constraints in our code design. Specifically, we handle the reliability constraint via an autoencoder, and handle the secrecy constraint with hash functions. For blocklengths smaller than or equal to 16, we evaluate through simulations the probability of error at the legitimate receiver and the leakage at the eavesdropper for our code construction. This leakage is defined as the mutual information between the confidential message and the eavesdropper's channel observations, and is empirically measured via a neural network-based mutual information estimator. Our simulation results provide examples of codes with positive secrecy rates that outperform the best known achievable secrecy rates obtained non-constructively for the Gaussian wiretap channel. Additionally, we show that our code design is suitable for the compound and arbitrarily varying Gaussian wiretap channels, for which the channel statistics are not perfectly known but only known to belong to a pre-specified uncertainty set. These models not only capture uncertainty related to channel statistics estimation, but also scenarios where the eavesdropper jams the legitimate transmission or influences its own channel statistics by changing its location.

I. INTRODUCTION

The wiretap channel [2] is a basic model to account for eavesdroppers in wireless communication. In this model, a sender (Alice) encodes a confidential message M into a codeword X^n and

V. Rana and R. Chou are with the Department of Electrical Engineering and Computer Science, Wichita State University, Wichita, KS. E-mails: vxrana@shockers.wichita.edu, remi.chou@wichita.edu. This work was supported in part by NSF grant CCF-2047913. Part of this work has been presented at the 2021 IEEE Information Theory Workshop [1]. This work has been submitted to the IEEE for possible publication. Copyright may be transferred without notice, after which this version may no longer be accessible.

transmits it to a legitimate receiver (Bob) over n uses of a channel in the presence of an external eavesdropper (Eve). Bob's estimate of M from his channel output observations is denoted by \hat{M} , and Eve's channel output observations are denoted by Z^n . In [2], the constraints are that Bob must be able to recover M , i.e., $\lim_{n \rightarrow \infty} \mathbb{P}[M \neq \hat{M}] = 0$, and the leakage about M at Eve, quantified by $I(M; Z^n)$, is not too large in the sense that $\lim_{n \rightarrow \infty} \frac{1}{n} I(M; Z^n) = 0$. Note that the stronger security requirement $\lim_{n \rightarrow \infty} I(M; Z^n) = 0$ can also be considered [3], meaning that Eve's observations Z^n are almost independent of M for large n . The secrecy capacity has been characterized for degraded discrete memoryless channels in [2], then for arbitrary discrete memoryless channels in [4], and then for Gaussian channels in [5].

While [2], [4], [5] provide non-constructive achievability schemes for the wiretap channel, constructive coding schemes have also been proposed. Specifically, coding schemes based on low-density parity-check (LDPC) codes [6]–[8], polar codes [9]–[12], and invertible extractors [13], [14] have been constructed for degraded and symmetric wiretap channel models. Moreover, the method in [13], [14] has been extended to the Gaussian wiretap channel [15]. Coding schemes based on random lattice codes have also been proposed for the Gaussian wiretap channel [16]. Subsequently, constructive [17]–[19] and random [20] polar coding schemes have been proposed to achieve the secrecy capacity of non-degraded discrete wiretap channels. A coding scheme that combines polar codes and invertible extractors has also been proposed to avoid the need for a pre-shared secret under strong secrecy [21]. All the references above consider the asymptotic regime, i.e., the regime where n approaches infinity. However, many practical applications require short packets or low latency. To fulfill this need, non-asymptotic and second order asymptotics achievability and converse bounds on the secrecy capacity of discrete and Gaussian wiretap channels have been established in [22]–[26]. Note that [22]–[26] focus on deriving fundamental limits and not on code constructions. We will review the works that are most related to our study and focus on code constructions at finite blocklength for the wiretap channel in Section II.

In this paper, we propose to design short blocklength codes (smaller than or equal to 16) for the Gaussian wiretap channel under information-theoretic security guarantees. Specifically, we quantify security in terms of the leakage $I(M; Z^n)$, i.e., the mutual information between the confidential message and the eavesdropper's channel observations. The main idea of our

approach is to decouple the reliability and secrecy constraints. Specifically, we use a deep learning approach based on a feed-forward neural network autoencoder [27] to handle the reliability constraint and cryptographic tools, namely, hash functions [28], to handle the secrecy constraint. Then, to evaluate the performance of our constructed code, we empirically estimate the leakage $I(M; Z^n)$. Note that even for small values of n this estimation is challenging with standard techniques such as binning of the probability space [29], k -nearest neighbor statistics [30], maximum likelihood estimation [31], or variational lower bounds [32]. Instead, to estimate the leakage, we use the neural network-based mutual information estimator MINE from [33], which is provably consistent and offers better performances than other known estimators in high dimension. We also compare the performances of our codes with the best known achievability and converse bounds on the maximal secrecy rate for the Gaussian wiretap channel [22].

We summarize the main features offered by our proposed code design as follows.

- 1) A modular approach that separates the code design in a secrecy layer and a reliability layer. The secrecy layer only deals with the secrecy constraint and only depends on the statistics of the eavesdropper's channel, whereas the reliability layer only deals with the reliability constraint and only depends on the statistics of the legitimate receiver's channel. This modular approach allows a simplified code design, for instance, if only one of the two layers needs to be (re)designed.
- 2) A precise control of the leakage through the independent, from the reliability layer, design of the secrecy layer. Indeed, as discussed next in Section II, deep learning approaches that seek to simultaneously design codes for reliability and secrecy do not seem to offer a good control on how small the leakage is.
- 3) A universal way of dealing with the secrecy constraint through the use of hash functions. This is beneficial, for instance, for compound [34], [35] and arbitrarily varying [36], [37] settings, as our results show that it becomes sufficient to design our code with respect to the best eavesdropper's channel. These models are particularly useful to capture uncertainty about the channel statistics of the eavesdropper channel or to model an active eavesdropper who can influence its channel statistics by changing location.
- 4) A method that can be applied to an arbitrary channel model as the conditional probability

distribution that defines the channel is not needed and only input and output channel samples are needed to design the reliability and secrecy layers.

- 5) A code design able to handle compound and arbitrarily varying settings when uncertainty holds on both the legitimate users' channel and the eavesdropper's channel, as demonstrated by our simulations results. Such settings are, for instance, relevant to model jamming from the eavesdropper.
- 6) As seen in our simulations, our code design provides examples of wiretap codes that outperform the best known achievable secrecy rates from [22] obtained non-constructively for the Gaussian wiretap channel.

The remaining of the paper is organized as follows. Section II reviews related works. Section III introduces the Gaussian wiretap channel model. Section IV describes our proposed code design and our simulation results for the Gaussian wiretap channel model. Section V discusses the compound and arbitrarily varying Gaussian wiretap channel models and presents our simulation results. Finally, Section VI provides concluding remarks.

II. RELATED WORKS

As elaborated on in the introduction, several code constructions have already been proposed for Gaussian wiretap channel coding in the asymptotic blocklength regime. Another challenging task is code designs in the finite blocklength regime. Next, we review known finite-length code constructions based on coding theoretic tools and deep learning tools in Sections II-A and II-B, respectively.

A. Works based on coding theory

In the following, we distinguish the works that consider a non-information-theoretic secrecy metric from the works that consider an information-theoretic secrecy metric.

1) *Non-information-theoretic secrecy metric*: A non-information-theoretic security metric called security gap, which is based on an error probability analysis at the eavesdropper, is used to evaluate the secrecy performance in [38]–[42]. Specifically, randomized convolutional codes for Gaussian and binary symmetric wiretap channels are studied in [38], and randomized

turbo codes for the Gaussian wiretap channel are investigated in [39]. Coding schemes for the Gaussian wiretap channel based on LDPC codes are proposed in [40], [41]. Additionally, another non-information-theoretic security approach called practical secrecy is investigated in [43], where a leakage between Alice’s message and an estimate of the message at Eve is estimated.

2) *Information-theoretic secrecy metric:* Next, we review works that consider the leakage $I(M; Z^n)$ as information-theoretic secrecy metric. In [44], punctured systematic irregular LDPC codes are proposed for the binary phase-shift-keyed-constrained Gaussian wiretap channel, and a leakage as low as 11 percent of the message length has been obtained for a blocklength $n = 10^6$. In [45], LDPC codes for the Gaussian wiretap channel have also been developed, and a leakage as low as 20 percent of the message length has been obtained for a blocklength $n = 50,000$. Most recently, in [46], randomized Reed-Muller codes are developed for the Gaussian wiretap channel, and a leakage as low as one percent of the message length has been obtained for a blocklength $n = 16$.

B. Works based on deep learning

Artificial neural networks (NNs) have gained attention in communication system design because their performance approaches the one of the state-of-the-art channel coding solutions. In [47], [48], neural networks (autoencoder) are used to learn the encoder and decoder for a channel coding task without secrecy constraints. Other machine learning approaches for channel coding without secrecy constraints have also been investigated in [49], [50] with reinforcement learning, in [51] with mutual information estimators, and in [52] with generative adversarial networks.

Recently, the autoencoder approach for channel coding has been extended to wiretap channel coding. In [53], [54], a coding scheme that imitates coset coding by clustering learned signal constellations is developed for the Gaussian wiretap channel under a non-information-theoretic secrecy metric, which relies on a cross-entropy loss function. In [55], a coding scheme for the Gaussian wiretap channel is developed under the information-theoretic leakage $I(M; Z^n)$ with an autoencoder approach that seeks to simultaneously optimized the reliability and secrecy constraints. A leakage as low as 15 percent of the message length is obtained in [55] for a blocklength $n = 16$. It seems that precisely controlling and minimizing the leakage is challenging

with such an approach. By contrast, in this paper, we propose an approach that separates the code design in a part that only deals with the reliability constraint (by means of an autoencoder) and in another part that only deals with the secrecy constraint (by means of hash functions). As supported by our simulation results, one of the advantages of our approach is a better control of how small the leakage can be made.

III. GAUSSIAN WIRETAP CHANNEL MODEL

Notation: Unless specified otherwise, capital letters represent random variables, whereas lowercase letters represent realizations of associated random variables, e.g., x is a realization of the random variable X . $|\mathcal{X}|$ denotes the cardinality of the set \mathcal{X} . $\|\cdot\|_2$ denotes the Euclidean norm. $\text{GF}(2^q)$ denotes a finite field of order 2^q , $q \in \mathbb{N}^*$.

Consider a memoryless Gaussian wiretap channel $(\mathcal{X}, P_{YZ|X}, \mathcal{Y} \times \mathcal{Z})$ defined by

$$Y \triangleq X + N_Y, \quad (1)$$

$$Z \triangleq X + N_Z, \quad (2)$$

where N_Y and N_Z are zero-mean Gaussian random variables with variances σ_Y^2 and σ_Z^2 , respectively. As formalized next, the objective of the sender is to transmit a confidential message M to a legitimate receiver by encoding it into a sequence X^n , which is then sent over n uses of the channels (1), (2) and yields the channel observations Y^n and Z^n at the legitimate receiver and eavesdropper, respectively.

Definition 1. Let $\mathbb{B}_0^n(\sqrt{nP})$ be the ball of radius \sqrt{nP} centered at the origin in \mathbb{R}^n under the Euclidian norm. An (n, k, P) code consists of

- a message set $\{0, 1\}^k$;
- an encoder $e : \{0, 1\}^k \rightarrow \mathbb{B}_0^n(\sqrt{nP})$, which, for a message $M \in \{0, 1\}^k$, forms the codeword $X^n \triangleq e(M)$;
- a decoder $d : \mathbb{R}^n \rightarrow \{0, 1\}^k$, which, from the channel observations Y^n , forms an estimate of the message as $d(Y^n)$.

The codomain of the encoder e reflects the power constraint $\|e(m)\|_2^2 \leq nP$, $\forall m \in \{0, 1\}^k$.

The performance of an (n, k, P) code is measured in terms of

- 1) The average probability of error $\mathbf{P}_e \triangleq \frac{1}{2^k} \sum_{m=1}^{2^k} \mathbb{P}[d(Y^n) \neq m | m \text{ is sent}]$;
- 2) The leakage at the eavesdropper $\mathbf{L}_e \triangleq I(M; Z^n)$.

Definition 2. An (n, k, P) code is said ϵ -reliable if $\mathbf{P}_e \leq \epsilon$ and δ -secure if $\mathbf{L}_e \leq \delta$. Moreover, a secrecy rate $\frac{k}{n}$ is said to be (ϵ, δ) -achievable with power constraint P if there exists an ϵ -reliable and δ -secure (n, k, P) code.

IV. CODING SCHEME

We first describe, at a high level, our coding scheme in Section IV-A. Specifically, our coding approach consists of two coding layers, one reliability layer, whose design is described in Sections IV-B, and one security layer, whose design is described in Section IV-C. Finally, we provide simulation results and examples of our code design for the Gaussian wiretap channel in Section IV-D.

A. High-level description of our coding scheme

Our code construction consists of (i) a reliability layer with an ϵ -reliable (n, q, P) code, described by the encoder/decoder pair (e_0, d_0) (this code is designed without any security requirement, i.e., its performance is solely measured in terms of average probability of error), and (ii) a security layer implemented with hash functions. We design the encoder/decoder pair (e_0, d_0) of the reliability layer using a deep learning approach based on neural network autoencoders as described in Section IV-B. We will then design two functions φ_s and f_s in Section IV-C to perform the encoding and decoding, respectively, at the secrecy layer. The encoder/decoder pair (e, d) for the encoding and decoding process of the reliability and secrecy layers considered jointly is described as follows:

Encoding: Assume that a fixed sequence of bits $s \in \mathcal{S} \triangleq \{0, 1\}^q \setminus \{\mathbf{0}\}$, called seed, is known to all parties. Alice generates a sequence B of $q - k$ bits uniformly at random in $\{0, 1\}^{q-k}$ (this sequence represents local randomness used to randomize the output of the function φ_s) and

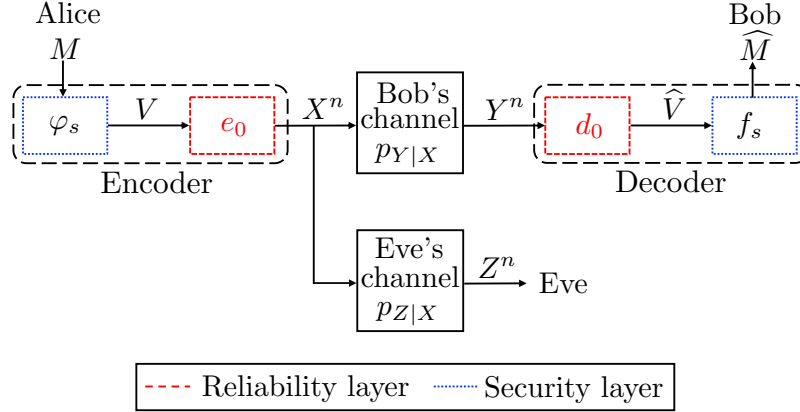


Figure 1: Our code design consists of a reliability layer and a security layer. The reliability layer is implemented using an autoencoder (e_0, d_0) described in Section IV-B, and the security layer is implemented using the functions φ_s and f_s described in Section IV-C1.

encodes the message $M \in \{0, 1\}^k$ as $e_0(\varphi_s(M, B))$. The overall encoding map e that describes the encoding at the secrecy and reliability layers is described by

$$e : \{0, 1\}^k \times \{0, 1\}^{q-k} \rightarrow \mathbb{B}_0^n(\sqrt{nP}),$$

$$(M, B) \mapsto e_0(\varphi_s(M, B)).$$

Decoding: Given Y^n and s , Bob decodes the message as $f_s(d_0(Y^n))$. The overall decoding map d that describes the decoding at the reliability and secrecy layers is

$$d : \mathbb{R}^n \rightarrow \{0, 1\}^k,$$

$$Y^n \mapsto f_s(d_0(Y^n)).$$

For a given code design, described by the encoder/decoder pair (e, d) , we will then evaluate the performance of this code by empirically measuring the leakage using a neural network-based mutual information estimator as described in Section IV-C2. Our code design is summarized in Figure 1.

Note that a coding strategy that separately handles the reliability and secrecy constraints is also used for the discrete wiretap channel in [13], [14], and for the Gaussian wiretap channel in [15]. In these works, an asymptotic regime is considered, i.e., the blocklength n tends to infinity, and

the security layer relies on the random choice of a hash function in a family of universal hash functions. In this paper, we also consider a family of hash functions for the security layer but only select a specific function in this family. This choice is deterministic and part of the coding scheme design as elaborated on in our simulation results.

B. Design of the reliability layer (e_0, d_0)

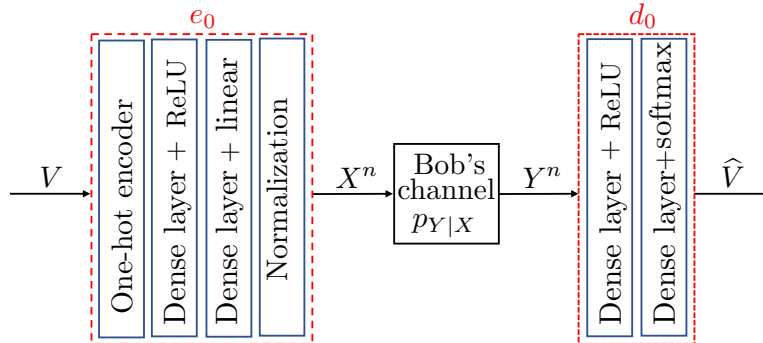


Figure 2: Architecture of the autoencoder (e_0, d_0) via feed-forward neural networks.

The design of the reliability layer consists in designing an ϵ -reliable (q, n, P) code described by the encoder/decoder pair (e_0, d_0) for the channel described by (1). Let $\mathcal{V} \triangleq \{1, 2, \dots, Q\}$ be the message set of this code where $Q \triangleq 2^q$. (e_0, d_0) is implemented by an autoencoder as in [47]. Specifically, the goal of the autoencoder is here to learn a representation of the encoded message that is robust to the channel noise, so that the received message at Bob can be reconstructed from its noisy channel observations with a small probability of error. Intuitively, as any error-correcting code, the autoencoder adds redundancy to the message to ensure recoverability by Bob in the presence of noise. As depicted in Figure 2, the encoder consists of (i) an embedding layer where the input $v \in \mathcal{V}$ is mapped to a one-hot vector $\mathbf{1}_v \in \mathbb{R}^Q$, i.e., a vector whose components are all equal to zero except the v -th component which is equal to one, followed by (ii) dense hidden layers that take v as input and return an n -dimensional vector, followed by (iii) a normalization layer that ensures that the average power constraint $\frac{1}{n} \|e_0(v)\|_2^2 \leq P$ is met for the codeword $e_0(v)$. Note that without loss of generality, one can assume that $P = 1$ since one can rewrite $\frac{1}{n} \|e_0(v)\|_2^2 \leq P$ as $\frac{1}{n} \|\tilde{e}_0(v)\|_2^2 \leq 1$, where $\tilde{e}_0(v) \triangleq e_0(v)/\sqrt{P}$. As depicted in Figure 2, the decoder consists of dense hidden layers and a softmax layer. More specifically,

let $\mu^{|\mathcal{V}|}$ be the output of the last dense layer in the decoder. The softmax layer takes $\mu^{|\mathcal{V}|}$ as input and returns a vector of probabilities $p^{|\mathcal{V}|} \in (0, 1)^{|\mathcal{V}|}$, where the entries p_v , $v \in \mathcal{V}$, are $p_v \triangleq \exp(\mu_v) \left(\sum_{i=1}^{|\mathcal{V}|} \exp(\mu_i) \right)^{-1}$. Finally, the decoded message \hat{v} corresponds to the index of $p^{|\mathcal{V}|}$ associated with the highest probability, i.e., $\hat{v} \in \arg \max_{v \in \mathcal{V}} p_v$. The autoencoder is trained over all possible messages $v \in \mathcal{V}$ using a stochastic gradient descent (SGD) [56] and the categorical cross-entropy loss function $L_{\text{loss}} \triangleq -\log(p_v)$.

C. Design of the security layer (φ_s, f_s)

The objective is now to design (φ_s, f_s) such that the total amount of leaked information about the original message is small in the sense that $I(M; Z^n) \leq \delta$, for some $\delta > 0$. For a given choice of (φ_s, f_s) , the performance of our code construction will be evaluated using a mutual information neural estimator (MINE) [33]. Before we describe the construction of (φ_s, f_s) , we review the definition of 2-universal hash functions.

Definition 3. [28] *Given two finite sets \mathcal{X} and \mathcal{Y} , a family \mathcal{G} of functions from \mathcal{X} to \mathcal{Y} is 2-universal if*

$$\forall x_1, x_2 \in \mathcal{X}, x_1 \neq x_2 \implies \mathbb{P}[G(x_1) = G(x_2)] \leq |\mathcal{Y}|^{-1},$$

where G is the random variable that represents the choice of a function $g \in \mathcal{G}$ uniformly at random in \mathcal{G} .

1) *Design of (φ_s, f_s) :* Let $\mathcal{S} \triangleq \{0, 1\}^q \setminus \{\mathbf{0}\}$. For $k \leq q$, consider the 2-universal hash family of functions $\mathcal{F} \triangleq \{f_s\}_{s \in \mathcal{S}}$, where for $s \in \mathcal{S}$,

$$\begin{aligned} f_s &: \{0, 1\}^q \rightarrow \{0, 1\}^k, \\ v &\mapsto (s \odot v)_k, \end{aligned}$$

where \odot is the multiplication in $\text{GF}(2^q)$ and $(\cdot)_k$ selects the k most significant bits. In our proposed code design, the security layer is handled via a specific function $f_s \in \mathcal{F}$ indexed by

the seed $s \in \mathcal{S}$. Then, we define

$$\begin{aligned} \varphi_s : \{0, 1\}^k \times \{0, 1\}^{q-k} &\rightarrow \{0, 1\}^q, \\ (m, b) &\mapsto s^{-1} \odot (m \| b), \end{aligned} \quad (3)$$

where $(\cdot \| \cdot)$ denotes the concatenation of two strings.

When the secrecy layer is combined with the reliability layer, our coding scheme can be summarized as follows. The input of the encoder e_0 is obtained by computing $V \triangleq \varphi_s(M, B)$, where $M \in \{0, 1\}^k$ is the message, and $B \in \{0, 1\}^{q-k}$ is a sequence of $q - k$ random bits generated uniformly at random. After computing V , the encoder e_0 , trained as described in Section IV-B, generates the codeword $X^n \triangleq e_0(V)$, which is sent over the channel by Alice. Bob and Eve observe Y^n and Z^n , respectively, as described by (1) and (2). The decoder d_0 , trained as described in Section IV-B, decodes Y^n as $\widehat{V} \triangleq d_0(Y^n)$. Then, the receiver performs the multiplication of \widehat{V} and s , which is followed by a selection of the k most significant bits to create an estimate of \widehat{M} of M , i.e., $\widehat{M} \triangleq f_s(\widehat{V})$.

2) *Leakage evaluation via Mutual Information Neural Estimator (MINE) [33]*: Let $\mathcal{F} \triangleq \{T_\theta\}_{\theta \in \Theta}$ be a set of functions parameterized by a deep neural network with parameters $\theta \in \Theta$. Define

$$I_\Theta(p_{MZ^n}) \triangleq \sup_{\theta \in \Theta} \mathbb{E}_{p_{MZ^n}} T_\theta(M, Z^n) - \log \mathbb{E}_{p_M p_{Z^n}} e^{T_\theta(M, Z^n)},$$

where p_{MZ^n} is the joint probability distribution of (M, Z^n) . By [33], $I_\Theta(p_{MZ^n})$ can approximate the mutual information $I(M; Z^n)$ with arbitrary accuracy. Note that because the true distribution p_{MZ^n} is unknown, one cannot directly use $I_\Theta(p_{MZ^n})$ to estimate $I(M; Z^n)$. However, by estimating the expectations in $I_\Theta(p_{MZ^n})$ with samples from p_{MZ^n} and p_M and p_{Z^n} , one can rewrite $I_\Theta(p_{MZ^n})$ as

$$\widehat{I}(M; Z^n) \triangleq \sup_{\theta \in \Theta} \frac{1}{k} \sum_{i=1}^k [T_\theta(m_i, z_i^n)] - \log \frac{1}{k} \sum_{i=1}^k [e^{T_\theta(\bar{m}_i, \bar{z}_i^n)}],$$

where the term $\frac{1}{k} \sum_{i=1}^k [T_\theta(m_i, z_i^n)]$ represents a sample mean using k samples $(m_i, z_i^n)_{i \in \{1, \dots, k\}}$ from p_{MZ^n} , and the term $\frac{1}{k} \sum_{i=1}^k [e^{T_\theta(\bar{m}_i, \bar{z}_i^n)}]$ represents a sample mean using k samples

$(\bar{m}_i, \bar{z}_i^n)_{i \in \{1, \dots, k\}}$ from $p_M p_{Z^n}$.

The goal of MINE, whose architecture is depicted in Figure 3, is to design T_θ such that $\hat{I}(M; Z^n)$ approaches the mutual information $I(M; Z^n)$. By [33], the estimator $\hat{I}(M; Z^n)$ converges to $I(M; Z^n)$ when the number of samples is sufficiently large [33]. Guidelines to implement the estimator $\hat{I}(M; Z^n)$ are also provided in [33].

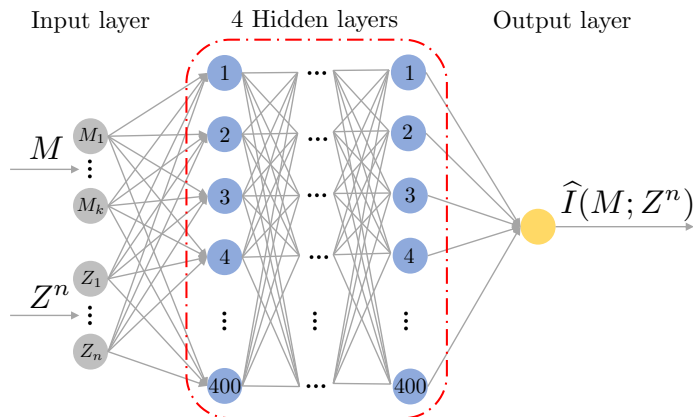
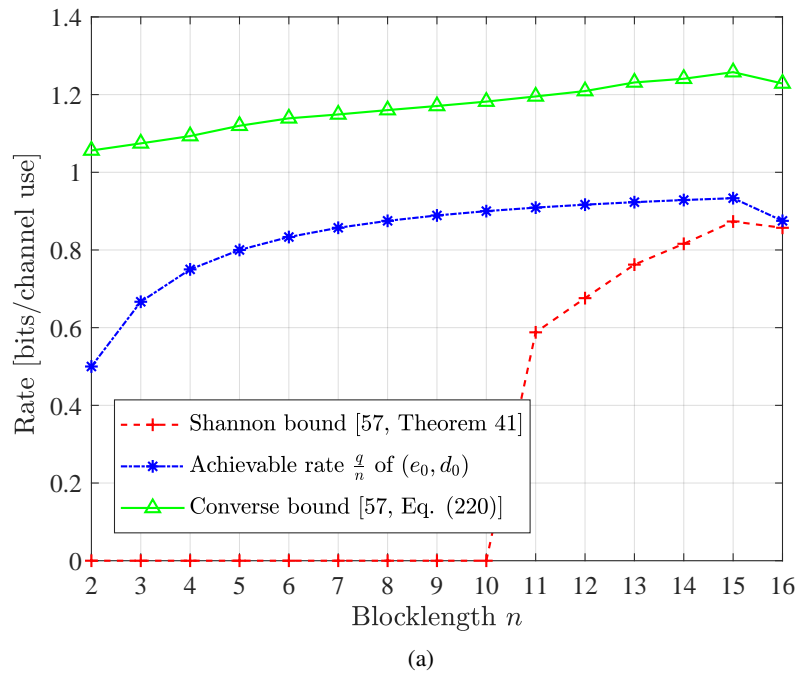


Figure 3: The security performance is evaluated in terms of the leakage $I(M; Z^n)$ via the mutual information estimator described in Section IV-C2, where $M \triangleq (M_i)_{i \in \{1, 2, \dots, k\}}$, $Z^n \triangleq (Z_j)_{j \in \{1, 2, \dots, n\}}$.

D. Simulations and examples of code designs

We now provide examples of code designs that follow the guidelines described in Sections IV-B, IV-C, and evaluate their performance in terms of average probability of error at Bob and leakage at Eve. The neural networks are implemented in Python 3.7 using Tensorflow 2.5.0.

1) *Autoencoder training for the design of the reliability layer (e_0, d_0)* : We consider the channel model (1) with $\sigma_Y^2 \triangleq 10^{-\text{SNR}_B/10}$ and $\text{SNR}_B = 9\text{dB}$, where, as explained in Section IV-B, without loss of generality, we choose $P = 1$. The autoencoder is trained for $q = n - 1$ using SGD with the Adam optimizer [56] at a learning rate of 0.001 over 600 epochs of 10^5 random encoder input messages with a batch size of 1000. Due to the exponential growth of the complexity with q , we changed the value of q to $n - 2$ when $n = 16$. Specifically, to evaluate $\mathbf{P}_e(e_0, d_0)$, we first generate the input $V \in \{0, 1\}^q$. Then, V is passed through the trained encoder e_0 , which generates the codewords X^n and the channel output Y^n . Finally, the trained decoder d_0 forms an estimate of V from Y^n .



n	$\mathbf{P}_e(e_0, d_0)$
2	$3.26 \cdot 10^{-5}$
3	$1.040 \cdot 10^{-4}$
4	$2.042 \cdot 10^{-4}$
5	$3.620 \cdot 10^{-4}$
6	$5.280 \cdot 10^{-4}$
7	$6.442 \cdot 10^{-4}$
8	$7.710 \cdot 10^{-4}$
9	$8.982 \cdot 10^{-4}$
10	$1.0438 \cdot 10^{-3}$
11	$1.2410 \cdot 10^{-3}$
12	$1.4864 \cdot 10^{-3}$
13	$2.0256 \cdot 10^{-3}$
14	$2.2706 \cdot 10^{-3}$
15	$2.8636 \cdot 10^{-3}$
16	$1.7192 \cdot 10^{-3}$

(b)

Figure 4: Figure 4a shows the rate versus the blocklength n obtained from $\epsilon \triangleq \mathbf{P}_e(e_0, d_0)$ listed in Figure 4b when $\text{SNR}_B = 9\text{dB}$.

Figure 4a compares the achievable rate $\frac{q}{n}$ of our reliability layer (e_0, d_0) with the best known achievability [57, Section III.J-4] and converse bounds [57, Section III.J-1] for channel coding. We observe that the rate of our reliability layer outperforms the achievability bounds from [57] for blocklengths smaller than or equal to 16 when $\text{SNR}_B = 9\text{dB}$. Note that for each value of n , this comparison is made for a given average probability of error $\mathbf{P}_e(e_0, d_0)$ as specified in Figure 4b.

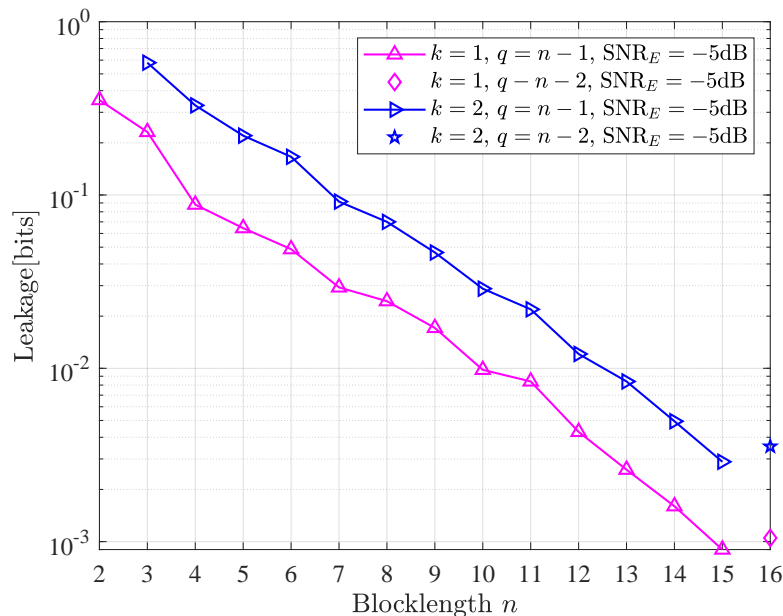


Figure 5: Leakage $\hat{I}(M; Z^n)$ versus blocklength. When $n \in \{2, 3, 4, \dots, 15\}$, $q = n - 1$, and when $n = 16$, $q = n - 2$.

2) *Design of the secrecy layer and leakage evaluation:* The seeds selected for the simulations are given in Table I. The seeds are picked at random for the values of n greater than eight, and multiple seeds have been tested for the values of n smaller than or equal to eight to minimize the leakage. The leakage is evaluated using MINE as follows. We used a fully connected feed-forward neural network with 4 hidden layers, each having 400 neurons and using rectified linear unit (ReLU) as activation function. The input layer has $k + n$ neurons, and the Adam optimizer with a learning rate of 0.001 is used for the training. The samples of the joint distribution p_{MZ^n} are produced via uniform generation of messages $M \in \{0, 1\}^k$ that are fed to the encoder

Table I: Selected seeds for the security layer.

n	seed s ($k = 1$)	seed s ($k = 2$)
2	1	-
3	11	11
4	010	010
5	1100	1100
6	00010	00011
7	001001	001001
8	0001101	0001101
9	10000000	10000000
10	100000000	100000000
11	1000000000	1000000000
12	10000000000	10000000000
13	100000000000	100000000000
14	1000000000000	1000000000000
15	10000000000000	10000000000000
16	100000000000000	100000000000000

$e = \varphi_s \circ e_0$, whose output X^n produces the channel output Z^n at Eve. The samples of the marginal distributions are generated by dropping either m or z^n from the joint samples (m, z^n) . We have trained the neural network over 10000 epochs of 20,000 messages with a batch size of 2500. Figure 5 shows the leakage versus the blocklength n for different values of k and $\text{SNR}_E = -5\text{dB}$. We observe that the leakage increases as k increases for fixed n and SNR_E , which is also supported by the following inequality on the leakage. When $k = 2$, if we write $M = (M_1, M_2)$, where $M_1, M_2 \in \{0, 1\}$, then by the chain rule and positivity of the mutual information, we have

$$\begin{aligned} I(M; Z^n) &= I(M_1; Z^n) + I(M_2; Z^n | M_1) \\ &\geq I(M_1; Z^n), \end{aligned}$$

where $I(M_1; Z^n)$ is interpreted as the leakage of a code with secrecy rate $\frac{1}{n}$ by considering that M_2 is a random bit part of B in (3).

3) *Average probability of error analysis:* To evaluate $\mathbf{P}_e(e, d)$, the trained encoder e_0 encodes the message $M \in \{0, 1\}^k$ as $e_0(\varphi_s(M, B))$, as described in Section IV-C, where $B \in \{0, 1\}^{q-k}$

is a sequence of $q - k$ random bits generated uniformly at random. The trained decoder d_0 forms $\widehat{M} \triangleq f_s(d_0(Y^n))$, as described in Section IV-C. Figure 6 shows $\mathbf{P}_e(e, d)$ versus the blocklength n . Note that we only plotted $\mathbf{P}_e(e, d)$ when $k = 1$ and $k = 2$ as an example, as one will always have $\mathbf{P}_e(e, d) \leq \mathbf{P}_e(e_0, d_0)$ for any value of k , since $e = \varphi_s \circ e_0$. From Figure 6, we also observe that, for fixed n, q , and $\text{SNR}_B = 9\text{dB}$, the probability of error decreases as k decreases, which is also supported by the following inequality

$$\mathbb{P}[(\widehat{M}_1, \widehat{M}_2) \neq (M_1, M_2)] \geq \mathbb{P}[\widehat{M}_1 \neq M_1],$$

where we have used the union bound and $\mathbb{P}[\widehat{M}_1 \neq M_1]$ is interpreted as the probability of error of a code with secrecy rate $\frac{1}{n}$ by considering that M_2 is a random bit part of B in (3).

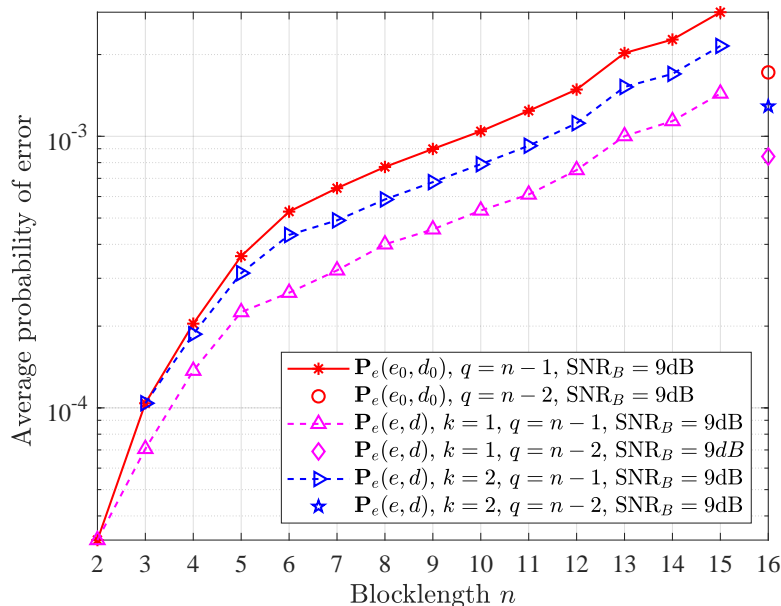
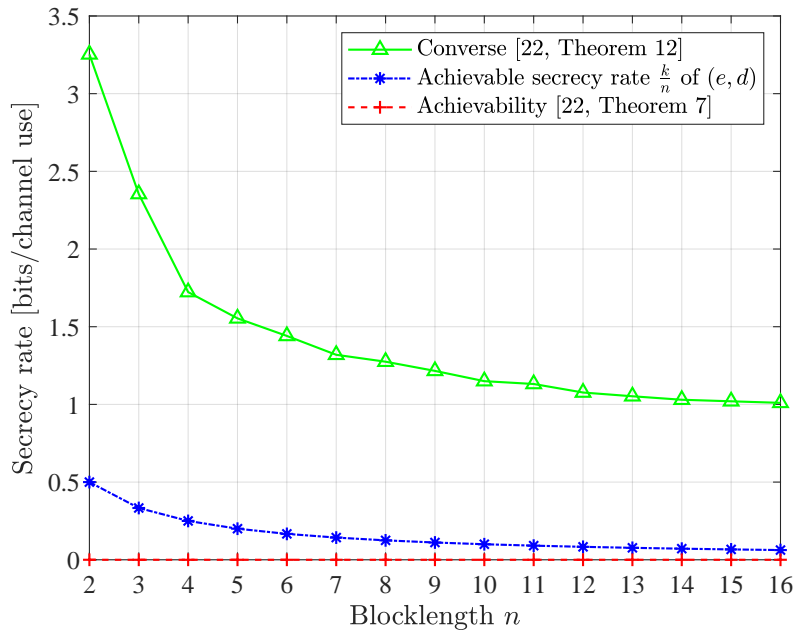


Figure 6: Average probability of error versus blocklength. When $n \in \{2, 3, 4, \dots, 15\}$, $q = n - 1$, and when $n = 16$, $q = n - 2$. During the training, the signal-to-noise ratio is $\text{SNR}_B = 9\text{dB}$.

4) *Discussion:* From Figures 5 and 6, we, for instance, see that for $\text{SNR}_B = 9\text{dB}$ and $\text{SNR}_E = -5\text{dB}$, we have designed codes that show that the secrecy rate $\frac{1}{10}$ is $(\epsilon = 5.330 \cdot 10^{-4}, \delta = 9.80 \cdot 10^{-3})$ -achievable with blocklength $n = 10$, and the secrecy rate $\frac{2}{13}$ is $(\epsilon =$



(a)

n	$\mathbf{P}_e(e, d)$ ($k = 1$)	$\widehat{I}(M; Z^n)$ ($k = 1$)
2	$3.26 \cdot 10^{-5}$	$3.5300 \cdot 10^{-1}$
3	$7.06 \cdot 10^{-5}$	$2.3100 \cdot 10^{-1}$
4	$1.370 \cdot 10^{-4}$	$8.800 \cdot 10^{-2}$
5	$2.252 \cdot 10^{-4}$	$6.440 \cdot 10^{-2}$
6	$2.654 \cdot 10^{-4}$	$4.870 \cdot 10^{-2}$
7	$3.208 \cdot 10^{-4}$	$2.930 \cdot 10^{-2}$
8	$4.000 \cdot 10^{-4}$	$2.200 \cdot 10^{-2}$
9	$4.542 \cdot 10^{-4}$	$1.710 \cdot 10^{-2}$
10	$5.330 \cdot 10^{-4}$	$9.80 \cdot 10^{-3}$
11	$6.104 \cdot 10^{-4}$	$8.40 \cdot 10^{-3}$
12	$7.510 \cdot 10^{-4}$	$4.30 \cdot 10^{-3}$
13	$1.0014 \cdot 10^{-3}$	$2.60 \cdot 10^{-3}$
14	$1.1376 \cdot 10^{-3}$	$1.16 \cdot 10^{-3}$
15	$1.4368 \cdot 10^{-3}$	$9.0 \cdot 10^{-4}$
16	$8.426 \cdot 10^{-4}$	$1.05 \cdot 10^{-3}$

(b)

Figure 7: Figure 7a shows the secrecy rate versus the blocklength n obtained from $\epsilon \triangleq \mathbf{P}_e(e, d)$ and $\delta \triangleq \widehat{I}(M; Z^n)$ listed in Figure 7b when $\text{SNR}_B = 9\text{dB}$ and $\text{SNR}_E = -5\text{dB}$.

$4.0700 \cdot 10^{-3}, \delta = 1.52 \cdot 10^{-3}$)-achievable with blocklength $n = 13$.

Figure 7a compares the achievable secrecy rate $\frac{k}{n}$ of our code design (e, d) with the best known achievability [22, Theorem 7] and converse bounds [22, Theorem 12] for the Gaussian wiretap channel, which are reviewed in the appendix for convenience. We observe that the rate of our code outperforms the best known achievability bounds for blocklengths smaller than or equal to 16 when $k = 1$, $\text{SNR}_B = 9\text{dB}$, and $\text{SNR}_E = -5\text{dB}$. Note that the best known upper bounds from [22] may not be optimal for small blocklengths, and improving them is an open problem. Note also that for each value of n , the comparison is made for a given average probability of error $\mathbf{P}_e(e, d)$ and leakage $\hat{I}(M; Z^n)$ as specified in Figure 7b.

V. COMPOUND AND ARBITRARILY VARYING WIRETAP CHANNEL MODELS

We first motivate the compound and arbitrarily varying wiretap channel models in Section V-A. We then formally describe these two models in Section V-B. We present our coding scheme design in Section V-C. Finally, we evaluate the performances of our code design through simulations for the compound and arbitrarily varying Gaussian wiretap channels in Sections V-D and V-E, respectively.

A. Background

In the setting of Section III, the channel statistics are assumed to be perfectly known to Alice and Bob and fixed during the entire transmission. However, in practice, the channel statistics may not be perfectly known due to the nature of the wireless channel and inaccuracy in estimating channel statistics. Further, in some scenarios, eavesdroppers could be active and influence their own channel statistics by changing location, or the statistics of Bob's channel through jamming. To model such scenarios two types of models have been introduced: compound wiretap channels and arbitrarily varying wiretap channels. For compound models, e.g., [34], [35], [58], [59], the channel statistics are fixed for all channel uses. Whereas for arbitrarily varying models, e.g., [36], [37], [58]–[60], the channel statistics may change in an unknown and arbitrary manner from channel use to channel use. Constructive coding schemes have also been proposed in [21] for the discrete compound and arbitrarily varying wiretap channels. While all the works above consider

the asymptotic regime, in this section, we design short blocklength codes for the compound and arbitrarily varying wiretap channel models.

B. Models

A compound or arbitrarily varying memoryless Gaussian wiretap channel $(\mathcal{X}, (P_{Y_i Z_j | X})_{i \in \mathcal{I}, j \in \mathcal{J}}, (\mathcal{Y}_i \times \mathcal{Z}_j)_{i \in \mathcal{I}, j \in \mathcal{J}})$ is defined for $i \in \mathcal{I}$, $j \in \mathcal{J}$ by

$$Y_i \triangleq X + N_{Y_i},$$

$$Z_j \triangleq X + N_{Z_j},$$

where N_{Y_i} and N_{Z_j} are zero mean Gaussian random variables with variances $\sigma_{Y_i}^2$ and $\sigma_{Z_j}^2$, respectively.

For the compound wiretap channel model, the channel statistics are constant throughout the transmission and are known to belong to given uncertainty sets \mathcal{I} , \mathcal{J} . The confidential message M is encoded into a transmitted sequence X^n , and Y_i^n and Z_j^n represent the corresponding received sequence at the legitimate receiver and eavesdropper, respectively for some $i \in \mathcal{I}$ and $j \in \mathcal{J}$.

Definition 4. A secrecy rate $\frac{k}{n}$ is said to be (ϵ, δ) -achievable with power constraint P for the compound wiretap channel if there exists a (n, k, P) code such that

$$\max_{i \in \mathcal{I}} \mathbf{P}_e^i(e, d) \leq \epsilon, \quad (4)$$

$$\max_{j \in \mathcal{J}} I(M; Z_j^n) \leq \delta, \quad (5)$$

where $\mathbf{P}_e^i(e, d) \triangleq \frac{1}{2^k} \sum_{m=1}^{2^k} \mathbb{P}[d(Y_i^n) \neq m | m \text{ is sent}]$.

In contrast to the compound wiretap channel, the channel statistics in arbitrarily varying wiretap channel models may vary in an unknown and arbitrary manner from channel use to channel use. Specifically, for the arbitrarily varying wiretap channel model, let $Y_{\mathbf{i}}^n$ and $Z_{\mathbf{j}}^n$ represent the corresponding received sequence at the legitimate receiver and eavesdropper, respectively for some $\mathbf{i} \in \mathcal{I}^n$ and $\mathbf{j} \in \mathcal{J}^n$.

Definition 5. A secrecy rate $\frac{k}{n}$ is said to be (ϵ, δ) -achievable with power constraint P for the arbitrarily varying wiretap channel if there exists a (n, k, P) code such that

$$\begin{aligned} \max_{\mathbf{i} \in \mathcal{I}^n} \mathbf{P}_e^{\mathbf{i}}(e, d) &\leq \epsilon, \\ \max_{\mathbf{j} \in \mathcal{J}^n} I(M; Z_{\mathbf{j}}^n) &\leq \delta, \end{aligned}$$

where $\mathbf{P}_e^{\mathbf{i}}(e, d) \triangleq \frac{1}{2^k} \sum_{m=1}^{2^k} \mathbb{P}[d(Y_{\mathbf{i}}^n) \neq m | m \text{ is sent}]$.

C. Coding scheme design

For the compound and the arbitrarily varying wiretap channels, the design of (e_0, d_0) for the reliability layer and (φ_s, f_s) for the secrecy layer is similar to Sections IV-B and IV-C, respectively. Specifically, we train the encoder/decoder pair for Bob's channel with noise variance $\sigma_{Y_{i^*}}^2 \triangleq \max_{i \in \mathcal{I}} \sigma_{Y_i}^2$, where $\sigma_{Y_i}^2 \triangleq 10^{-\text{SNR}_B(i)/10}$, $i \in \mathcal{I}$. In other words, the reliability layer is designed for the worse, in terms of signal-to-noise ratio, Bob's channel. Note also that, during the training phase, the noise variance is fixed for all the channel uses. Then, we optimize the seed s by minimizing the leakage for Eve's channel with noise variance $\sigma_{Z_{j^*}}^2 \triangleq \min_{j \in \mathcal{J}} \sigma_{Z_j}^2$, where $\sigma_{Z_j}^2 \triangleq 10^{-\text{SNR}_E(j)/10}$, $j \in \mathcal{J}$. In other words, the secrecy layer is designed for the best, in terms of signal-to-noise ratio, Eve's channel. This optimized seed s is then used by the encoder/decoder pair $(e, d) = (e_0 \circ \varphi_s, f_s \circ d_0)$, from which we evaluate $(\mathbf{P}_e^i(e, d), I(M; Z_j^n))$, $i \in \mathcal{I}$, $j \in \mathcal{J}$, and $(\mathbf{P}_e^{\mathbf{i}}(e, d), I(M; Z_{\mathbf{j}}^n))$, $\mathbf{i} \in \mathcal{I}^n$, $\mathbf{j} \in \mathcal{J}^n$ in Sections V-D, V-E.

D. Simulations and examples of code designs for the compound wiretap channel

1) *Average probability of error analysis:* In our simulations, we consider $\mathcal{I} = \{1, 2\}$ and $\text{SNR}_B(i) \in \{9, 10\}$ dB, $i \in \mathcal{I}$. We evaluate the average probability of error $\mathbf{P}_e^i(e, d)$ for $i \in \mathcal{I}$ as follows. The autoencoder is trained at $\text{SNR}_B(i^*) = 9$ dB, where $i^* = 1$. The message $M \in \{0, 1\}^k$ generated uniformly at random is passed through the trained encoder e_0 , which generates the codewords X^n and the channel output $Y_i^n \triangleq X^n + N_{Y_i}^n$, $i \in \mathcal{I}$, where $N_{Y_i} \sim \mathcal{N}(0, \sigma_{Y_i}^2)$. Then, the trained decoder d_0 forms an estimate \widehat{M}_i , $i \in \mathcal{I}$. Here, $\sigma_{Y_i}^2$ is fixed for the entire duration of the transmission. We use 5×10^6 random messages to evaluate the average probability of error. Figure 8 shows the average probability of error $\mathbf{P}_e^i(e, d)$ when $k = 1$ and $\text{SNR}_B(i^* = 1) = 9$ dB

and $\text{SNR}_B(i = 2) = 10\text{dB}$, respectively. We observe from Figure 8 that it is sufficient to design our code for the worst signal-to-noise ratio for Bob, i.e., $\text{SNR}_B(i^*) = 9\text{dB}$. In particular, we observe that, irrespective of what the actual channel is, Bob is able to decode the message with a probability of error smaller than or equal to $\mathbf{P}_e^{i^*=1}(e, d)$.

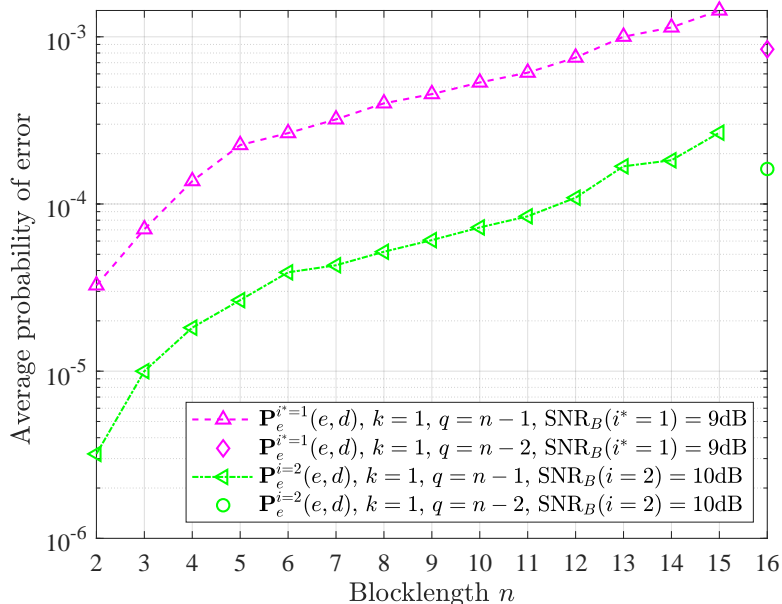


Figure 8: Average probability of error versus blocklength n .

2) *Leakage evaluation*: For the simulations, we consider $\mathcal{J} = \{1, 2, 3\}$ and $\text{SNR}_E(j) \in \{-8, -6.5, -5\}\text{dB}$, $j \in \mathcal{J}$. We compute the leakage $I(M; Z_j^n)$ for $j \in \mathcal{J}$ as in Section IV-D2. The message $M \in \{0, 1\}^k$ is passed through the trained encoder e_0 , which generates the codewords X^n , and the channel output at Eve is $Z_j^n \triangleq X^n + N_{Z_j^n}$, $j \in \mathcal{J}$, where $N_{Z_j} \sim \mathcal{N}(0, \sigma_{Z_j}^2)$. The noise variance $\sigma_{Z_j}^2$ is fixed for the entire duration of the transmission. Figure 9 shows the estimated mutual information $\hat{I}(M; Z_j^n)$, at $\text{SNR}_E(j = 1) = -8\text{dB}$, $\text{SNR}_E(j = 2) = -6.5\text{dB}$, and $\text{SNR}_E(j^* = 3) = -5\text{dB}$. From Figure 9, we observe that it is sufficient to design our code for the best signal-to-noise ratio, i.e., $\text{SNR}_E(j^*) = -5\text{dB}$. In particular, we see that, irrespective of what the actual eavesdropper's channel is, we always

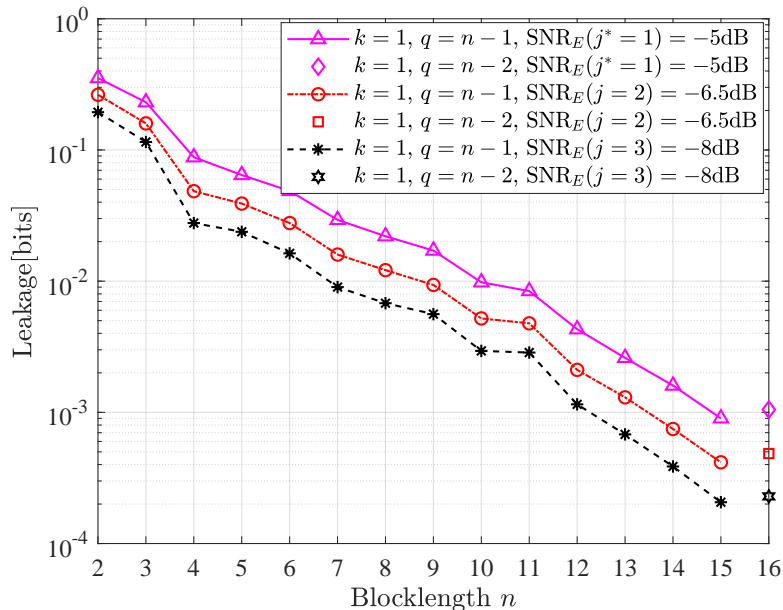


Figure 9: Leakage $\hat{I}(M; Z_j^n)$ versus blocklength n .

achieve a leakage smaller than or equal to $\hat{I}(M; Z_{j^*}^n)$, which is also supported by the following inequality on the leakage. For $j \in \mathcal{J}$ and $j^* \in \arg \min_{j \in \mathcal{J}} \sigma_{Z_j}^2$, we have

$$\begin{aligned}
 I(M; Z_j^n) &\leq I(M; Z_j^n Z_{j^*}^n) \\
 &= I(M; Z_{j^*}^n) + I(M; Z_j^n | Z_{j^*}^n) \\
 &= I(M; Z_{j^*}^n),
 \end{aligned}$$

where the first inequality holds by the chain rule and positivity of the mutual information, the first equality holds by the chain rule, and the last equality holds because, without loss of generality, one can redefine Z_j^n such that $Z_j^n = Z_{j^*}^n + N^n$, where $N \sim \mathcal{N}(0, \sigma_{Z_j}^2 - \sigma_{Z_{j^*}}^2)$, i.e., $M - Z_j^n - Z_{j^*}^n$ forms a Markov chain, since the distributions $p_{X^n Z_j^n}$ and $p_{X^n Z_{j^*}^n}$ are preserved and the constraints (4) and (5) of the problem do not depend on the joint distribution $p_{Z_j^n Z_{j^*}^n}$.

As an example, from Figure 8 and 9, we see that for $\text{SNR}_B = 10\text{dB}$ and $\text{SNR}_E = -8\text{dB}$, we have designed codes that show that the secrecy rate $\frac{1}{8}$ is $(\epsilon = 5.18 \cdot 10^{-5}, \delta = 6.80 \cdot 10^{-3})$ -

achievable with blocklength $n = 8$.

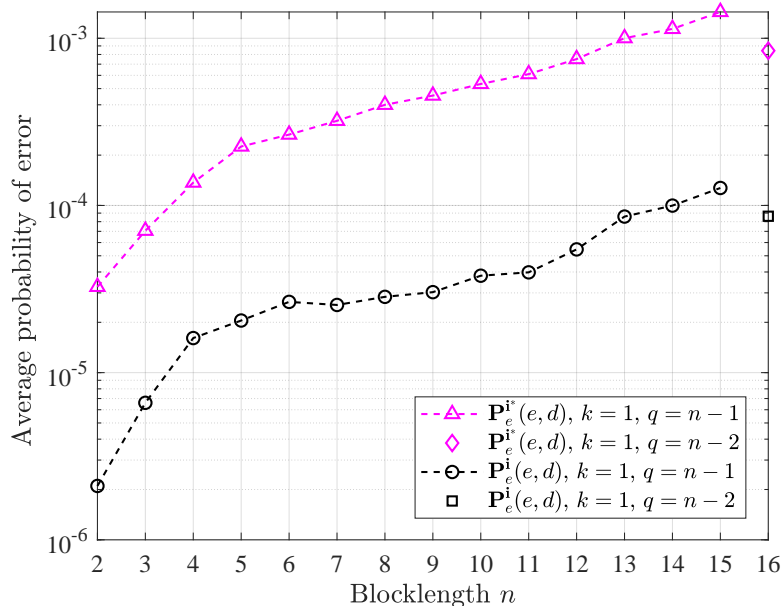


Figure 10: Average probability of error versus blocklength n when $k = 1$ and training $\text{SNR}_B(i^*) = 9\text{dB}$.

E. Simulations and examples of code designs for the arbitrarily varying wiretap channel

1) *Average probability of error analysis:* For the arbitrarily varying channel, we evaluate the probability of error $P_e^i(e, d)$, $\mathbf{i} \in \mathcal{I}^n$ for $k = 1$ in Figure 10 as follows. We consider $\mathcal{I} = \{1, 2, 3, \dots, 31\}$ and $\text{SNR}_B(i) \in \{9, 9.1, 9.2, \dots, 12\}$, $i \in \mathcal{I}$. The autoencoder is trained at $\text{SNR}_B(i^* = 1) = 9\text{dB}$, where the noise variance is fixed for the entire duration of the transmission. The message $M \in \{0, 1\}^k$ generated uniformly at random is passed through the trained encoder e_0 , which generates the codewords X^n and the channel output at Bob $Y_i^n \triangleq X^n + N_{Y_i^n}$, $\mathbf{i} \in \mathcal{I}^n$. Then, the trained decoder d_0 forms an estimate \widehat{M}_i , $\mathbf{i} \in \mathcal{I}^n$. Here, $N_{Y_i^n}$ is a length n vector whose variance of each component is picked uniformly at random from the known uncertainty set $\{10^{-12\text{dB}/10}, 10^{-11.9\text{dB}/10}, 10^{-11.8\text{dB}/10}, \dots, 10^{-9\text{dB}/10}\}$. For our simulations, the variance of the noise vector $N_{Y_i^n}$ is fixed for every 50,000 codewords. The autoencoder is tested with 5×10^6 random messages for $n > 10$ and with 10^7 random messages for $n \leq 10$.

Figure 10 shows that even though there is a mismatch between the training signal-to-noise ratio of the encoder/decoder pair and the actual channel, Bob is still able to decode the message with a probability of error smaller than or equal to $\mathbf{P}_e^{\mathbf{i}^*}(e, d)$, where \mathbf{i}^* is a vector made of n repetitions of i^* .

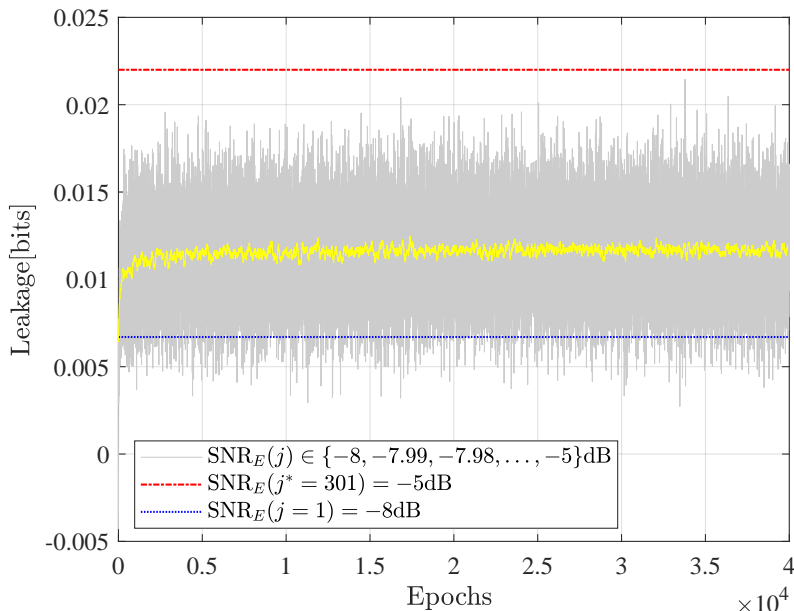


Figure 11: Example of leakage $\hat{I}(M; Z_j^n)$ versus epochs when $k = 1$, $n = 8$, $q = n - 1$, $s = 001101$, and $j \in \{1, 2, 3, \dots, 301\}$. The grey curve represents the estimated leakage by a mutual information neural estimator and the yellow curve represents the 100-sample moving average of $\hat{I}(M; Z^n)$. The red and blue curves represent the estimated leakage for $\text{SNR}_E(j^* = 301) = -5\text{dB}$ and $\text{SNR}_E(j = 1) = -8\text{dB}$, respectively, after convergence.

2) *Leakage evaluation:* For the arbitrarily varying channel, we evaluate the leakage $I(M; Z_j^n)$, for $\mathbf{j} \in \mathcal{J}^n$ as in Section IV-D2. The channel output at Eve is $Z_j^n \triangleq X^n + N_{Z_j^n}$, $\mathbf{j} \in \mathcal{J}^n$. In Figure 11, we consider $\mathcal{J} = \{1, 2, 3, \dots, 301\}$ and $\text{SNR}_E(j) \in \{-8, -7.99, -7.98, \dots, -5\}\text{dB}$, $j \in \mathcal{J}$. Figure 11 shows the estimated mutual information $\hat{I}(M; Z_j^n)$ when $k = 1$ and $n = 8$, where the variance of the noise vector $N_{Z_j^n}$ is fixed for 20,000 codewords per epoch. Here, $N_{Z_j^n}$ is a length n vector whose variance of each component is picked uniformly at random from the known uncertainty set $\{10^{5\text{dB}/10}, 10^{5.01\text{dB}/10}, 10^{5.02\text{dB}/10}, \dots, 10^{8\text{dB}/10}\}$. We can see from Figure 11 that it is sufficient to design our code for the best signal-to-noise ratio, i.e., $\text{SNR}_E(j^* = 301) =$

−5dB. In particular, we observe that, regardless of what the actual channel is, we always achieve a leakage smaller than or equal to $\widehat{I}(M; Z_{\mathbf{j}^*}^n)$, where \mathbf{j}^* is a vector made of n repetitions of j^* , which is also supported by the following inequality on the leakage.

For any $\mathbf{j} \in \mathcal{J}^n$, we have

$$I(M; Z_{\mathbf{j}}^n) \leq I(M; Z_{\mathbf{j}^*}^n),$$

because, similar to the compound setting, without loss of generality, one can redefine $Z_{\mathbf{j}}^n$ such that $M - Z_{\mathbf{j}}^n - Z_{\mathbf{j}^*}^n$ forms a Markov chain.

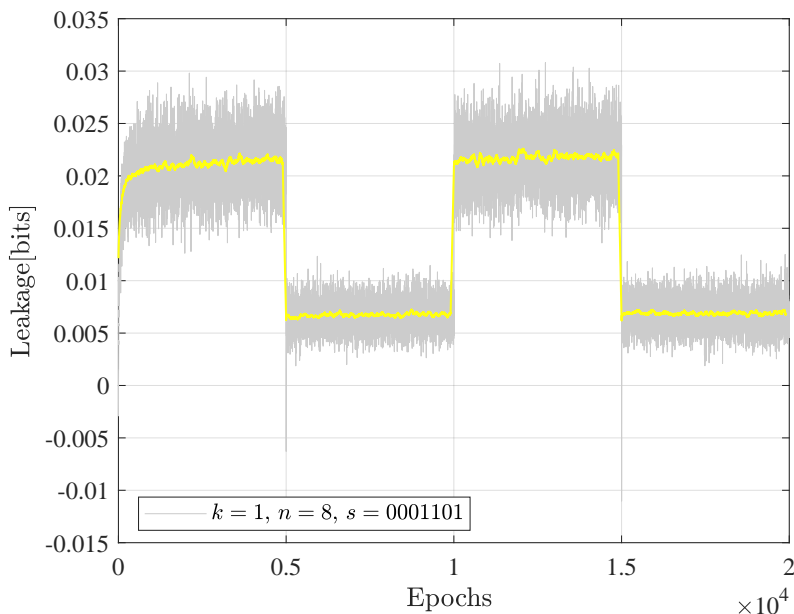


Figure 12: Example of leakage $\widehat{I}(M; Z_{\mathbf{j}}^n)$ versus epochs when $q = n - 1$ and $\text{SNR}_E(j) \in \{-8, -5\}$, $j \in \{1, 2\}$. The yellow curve represents the 100-sample moving average of $\widehat{I}(M; Z^n)$.

Figure 12 shows the estimated mutual information $\widehat{I}(M; Z_{\mathbf{j}}^n)$ for $k = 1$ and $n = 8$, when $\text{SNR}_E \in \{-8, -5\}$ dB. Here, each component of the noise vector $N_{Z_{\mathbf{j}}^n}$ has fixed variance, which alternatively takes the values $10^{5\text{dB}/10}$ and $10^{8\text{dB}/10}$, for every 5000 epochs with 20,000 codewords per epoch. In other words, each component of the noise vector has variance $10^{5\text{dB}/10}$ for the first 5000 epochs, then $10^{8\text{dB}/10}$ for the next 5000 epochs, and so on. Again, we observe that it is

sufficient to consider the worst case for the code design, since the leakage is always upper bounded by the leakage obtained for the best eavesdropper's signal-to-noise ratio, i.e., when $\text{SNR}_E = -5\text{dB}$.

VI. CONCLUDING REMARKS

We designed short blocklength codes for the Gaussian wiretap channel under an information-theoretic secrecy metric. Our approach consisted in decoupling the reliability and secrecy constraints to offer a simple and modular code design, and to precisely control how small the leakage is. Specifically, we handled the reliability constraint via an autoencoder and the secrecy constraint via hash functions. We evaluated the performance of our code design through simulations in terms of probability of error at the legitimate receiver and leakage at the eavesdropper for blocklengths smaller than or equal to 16. Our results provide examples of code designs that outperform the best known achievable secrecy rates obtained non-constructively for the Gaussian wiretap channel. We highlight that our code design method can be applied to any channels since it does not require the knowledge of the channel model but only the knowledge of input and output channel samples. We also showed that our code design is applicable to settings where uncertainty holds on the channel statistics, e.g., compound wiretap channels, and arbitrarily varying wiretap channels.

APPENDIX

A. Achievability bound for the Gaussian wiretap channel

The maximal secrecy rate $R_s(n, \epsilon, \delta)$ achievable by an ϵ -reliable and δ -secure (n, k, P) code is lower bounded as [22, Theorem 7 and Section IV.C-1]

$$R_s(n, \epsilon, \delta) \geq \frac{1}{n} \log_2 \frac{M(\epsilon, n)}{L(n, \delta)},$$

with $M(\epsilon, n)$ the number of codewords for a probability of error ϵ and blocklength n inferred by Shannon's channel coding achievability bound [57, Section III.J-4], and $L(n, \delta)$ such that

$$\sqrt{L(n, \delta)} \triangleq \min_{\gamma} \frac{\sqrt{\gamma \mathbb{E}[\exp(-|B_n - \log \gamma|)]}}{2(\delta + \mathbb{E}[\exp(-|B_n - \log \gamma|^+)] - 1)},$$

where the minimization is over all $\gamma > 0$ such that the denominator is positive, and

$$B_n \triangleq \frac{n}{2} \log_2 \left(1 + \frac{P}{\sigma_Z^2} \right) + \frac{\log_2 e}{2} \sum_{t=1}^n \left(1 - \frac{(\sqrt{P}Z_t - \sqrt{\sigma_Z^2})^2}{P + \sigma_Z^2} \right),$$

where $Z_t, t \in \{1, \dots, n\}$, represents the t^{th} i.i.d copy of Z defined in (2).

B. Converse bound for the Gaussian wiretap channel

Let $Q_{Y|Z} : \mathcal{Y} \rightarrow \mathcal{Z}$ be an arbitrary random transformation and P_{XZ} be a probability distribution on $\mathcal{X} \times \mathcal{Z}$. An ϵ -reliable and δ -secure (n, k, P) code for the wiretap channel $(\mathcal{X}, P_{YZ|X}, \mathcal{Y} \times \mathcal{Z})$ satisfies [22, Theorem 12 and Section IV.C-3]

$$2^k \leq \inf_{\tau \in (0, 1-\epsilon-\delta)} \frac{\tau + \delta}{\tau \beta_{1-\epsilon-\delta-\tau}(P_{X^n Y^n Z^n}, P_{X^n Z^n} Q_{Y^n|Z^n})},$$

where P_{XYZ} denotes the joint probability distribution induced by the code and

$$\beta_{1-\epsilon-\delta-\tau}(P_{X^n Y^n Z^n}, P_{X^n Z^n} Q_{Y^n|Z^n}) = \mathbb{P}[\bar{D}_n \geq \bar{\gamma}],$$

where

$$\begin{aligned} \bar{D}_n &\triangleq nC_s \\ &+ \frac{\log_2 e}{2} \sum_{t=1}^n \left(\frac{N_{Z_t}^2}{\sigma_Z^2} - \frac{(\bar{N}_{Z_t} - c_0(N_{Z_t} + \sqrt{P}))^2}{P + \sigma_Z^2} + \frac{\bar{N}_{Z_t}^2}{P + \sigma_Y^2} + \frac{(c_1 N_{Z_t} + c_0 \bar{N}_{Z_t} - c_0^2 \sqrt{P})^2}{\sigma_Y^2} \right), \end{aligned}$$

with $N_{Z_t} \sim \mathcal{N}(0, \sigma_Z^2)$, $\bar{N}_{Z_t} \sim \mathcal{N}(0, P + \sigma_Y^2)$, and $c_0 \triangleq \sqrt{\frac{\sigma_Z^2 - \sigma_Y^2}{P + \sigma_Z^2}}$, $c_1 \triangleq \sqrt{\frac{P + \sigma_Y^2}{P + \sigma_Z^2}}$, and the threshold $\bar{\gamma}$ satisfies $\mathbb{P}[\bar{B}_n \geq \bar{\gamma}] = 1 - \epsilon - \delta$ with

$$\bar{B}_n \triangleq nC_s + \frac{\log_2 e}{2} \sum_{t=1}^n \left(\frac{(N_{Y_t} + \bar{N}_{Y_t})^2}{\sigma_Z^2} - \frac{N_{Y_t}^2}{\sigma_Y^2} + \frac{(\sqrt{P} + N_{Y_t})^2}{P + \sigma_Y^2} - \frac{(\sqrt{P} + N_{Y_t} + \bar{N}_{Y_t})^2}{P + \sigma_Z^2} \right),$$

where $Y_t, t \in \{1, \dots, n\}$, represents the t^{th} i.i.d copy of Y defined in (1), $N_{Y_t} \sim \mathcal{N}(0, \sigma_Y^2)$, and $\bar{N}_{Y_t} \sim \mathcal{N}(0, \sigma_Z^2 - \sigma_Y^2)$.

REFERENCES

- [1] V. Rana and R. A. Chou, "Design of short blocklength wiretap channel codes: Deep learning and cryptography working hand in hand," in *IEEE Inf. Theory Workshop*, 2021, pp. 1–6.

- [2] A. Wyner, "The wire-tap channel," *The Bell System Technical Journal*, vol. 54, no. 8, pp. 1355–1387, 1975.
- [3] U. Maurer and S. Wolf, "Information-theoretic key agreement: From weak to strong secrecy for free," in *Lecture Notes in Computer Science*, 2000, pp. 351–368.
- [4] I. Csiszar and J. Korner, "Broadcast channels with confidential messages," *IEEE Trans. Inf. Theory*, vol. 24, no. 3, pp. 339–348, 1978.
- [5] S. Cheong and M. Hellman, "The Gaussian wire-tap channel," *IEEE Trans. Inf. Theory*, vol. 24, no. 4, pp. 451–456, 1978.
- [6] A. Thangaraj, S. Dihidar, A. Calderbank, S. W. McLaughlin, and J. Merolla, "Applications of LDPC codes to the wiretap channel," *IEEE Trans. Inf. Theory*, vol. 53, no. 8, pp. 2933–2945, 2007.
- [7] A. Subramanian, A. Thangaraj, M. B. Bloch, and S. McLaughlin, "Strong secrecy on the binary erasure wiretap channel using large-girth LDPC codes," *IEEE Trans. Inf. Forensics and Security*, vol. 6, no. 3, pp. 585–594, 2011.
- [8] V. Rathi, R. Urbanke, M. Andersson, and M. Skoglund, "Rate-equivocation optimal spatially coupled LDPC codes for the BEC wiretap channel," in *IEEE Int. Symp. Inf. Theory*, 2011, pp. 2393–2397.
- [9] H. Mahdaviifar and A. Vardy, "Achieving the secrecy capacity of wiretap channels using polar codes," *IEEE Trans. Inf. Theory*, vol. 57, no. 10, pp. 6428–6443, 2011.
- [10] E. Şaşoğlu and A. Vardy, "A new polar coding scheme for strong security on wiretap channels," in *IEEE Int. Symp. Inf. Theory*, 2013, pp. 1117–1121.
- [11] M. Andersson, R. Schaefer, T. Oechtering, and M. Skoglund, "Polar coding for bidirectional broadcast channels with common and confidential messages," *IEEE J. Selected Areas Commun.*, vol. 31, no. 9, pp. 1901–1908, 2013.
- [12] M. Andersson, V. Rathi, R. Thobaben, J. Kliewer, and M. Skoglund, "Nested polar codes for wiretap and relay channels," *IEEE Commun. Letters*, vol. 14, no. 8, pp. 752–754, 2010.
- [13] M. Hayashi and R. Matsumoto, "Construction of wiretap codes from ordinary channel codes," in *IEEE Int. Symp. Inf. Theory*, 2010, pp. 2538–2542.
- [14] M. Bellare, S. Tessaro, and A. Vardy, "Semantic security for the wiretap channel," in *Advances of cryptology. Springer*, 2012, pp. 294–311.
- [15] H. Tyagi and A. Vardy, "Explicit capacity-achieving coding scheme for the Gaussian wiretap channel," in *IEEE Int. Symp. Inf. Theory*, 2014, pp. 956–960.
- [16] C. Ling, L. Luzzi, J. Belfiore, and D. Stehlé, "Semantically secure lattice codes for the Gaussian wiretap channel," *IEEE Trans. Inf. Theory*, vol. 60, no. 10, pp. 6399–6416, 2014.
- [17] Y. Wei and S. Ulukus, "Polar coding for the general wiretap channel with extensions to multiuser scenarios," *IEEE J. Selected Areas Commun.*, vol. 34, no. 2, pp. 278–291, 2016.
- [18] R. Chou and M. Bloch, "Polar coding for the broadcast channel with confidential messages: A random binning analogy," *IEEE Trans. Inf. Theory*, vol. 62, no. 5, pp. 2410–2429, 2016.
- [19] J. Renes, R. Renner, and D. Sutter, "Efficient one-way secret-key agreement and private channel coding via polarization," in *Advances in Cryptology. Springer*, 2013, pp. 194–213.
- [20] T. C. Gulcu and A. Barg, "Achieving secrecy capacity of the wiretap channel and broadcast channel with a confidential component," vol. 63, no. 2, 2017, pp. 1311–1324.
- [21] R. A. Chou, "Unified framework for polynomial-time wiretap channel codes," *arXiv preprint arXiv:2002.01924*, 2020.

- [22] W. Yang, R. Schaefer, and H. Poor, "Wiretap channels: Nonasymptotic fundamental limits," *IEEE Trans. Inf. Theory*, vol. 65, no. 7, pp. 4069–4093, 2019.
- [23] M. Hayashi, "Tight exponential analysis of universally composable privacy amplification and its applications," *IEEE Trans. Inf. Theory*, vol. 59, no. 11, pp. 7728–7746, 2013.
- [24] V. Tan, "Achievable second-order coding rates for the wiretap channel," in *IEEE Int. Conf. Commun. Systems*, 2012, pp. 65–69.
- [25] M. Hayashi, H. Tyagi, and S. Watanabe, "Strong converse for a degraded wiretap channel via active hypothesis testing," in *Annual Allerton Conf. Commun., Control, and Computing*, 2014, pp. 148–151.
- [26] V. Tan and M. Bloch, "Information spectrum approach to strong converse theorems for degraded wiretap channels," *IEEE Trans. Inf. Forensics and Security*, vol. 10, no. 9, pp. 1891–1904, 2015.
- [27] I. Goodfellow, Y. Bengio, and A. Courville, *Deep learning*. MIT press, 2016.
- [28] J. Carter and M. Wegman, "Universal classes of hash functions," *J. Computer and System Sciences*, vol. 18, no. 2, pp. 143–154, 1979.
- [29] G. Darbellay and I. Vajda, "Estimation of the information by an adaptive partitioning of the observation space," *IEEE Trans. Inf. Theory*, vol. 45, no. 4, pp. 1315–1321, 1999.
- [30] A. Kraskov, H. Stögbauer, and P. Grassberger, "Estimating mutual information," *Physical Review E*, vol. 69, no. 6, pp. 066138(1–16), 2004.
- [31] T. Suzuki, M. Sugiyama, J. Sese, and T. Kanamori, "Approximating mutual information by maximum likelihood density ratio estimation," in *Workshop on New Challenges for Feature Selection in Data Mining and Knowledge Discovery*, 2008, pp. 5–20.
- [32] D. Barber and F. Agakov, "The IM algorithm: A variational approach to information maximization," in *Int. Conf. Neural Inf. Processing Systems*, 2003, pp. 201–208.
- [33] M. I. Belghazi, A. Baratin, S. Rajeswar, S. Ozair, Y. Bengio, A. Courville, and R. D. Hjelm, "MINE: Mutual information neural estimation," *arXiv preprint arXiv:1801.04062*, 2018.
- [34] Y. Liang, G. Kramer, H. Poor, and S. Shamai, "Compound wiretap channels," *EURASIP J. Wirel. Commun. Netw.*, no. 142374, 2009.
- [35] I. Bjelakovic, H. Boche, and J. Sommerfeld, "Secrecy results for compound wiretap channels," *Problems Inf. Transmission*, vol. 49, no. 1, pp. 73–98, 2013.
- [36] —, "Capacity results for arbitrarily varying wiretap channels," in *Inf. Theory, Combinatorics, and Search Theory*, 2013, pp. 123–144.
- [37] E. MolavianJazi, M. Bloch, and J. Laneman, "Arbitrary jamming can preclude secure communication," in *Annual Allerton Conf. Commun., Control, and Computing*, 2009, pp. 1069–1075.
- [38] A. Nooraiepour and T. Duman, "Randomized convolutional codes for the wiretap channel," *IEEE Trans. Commun.*, vol. 65, no. 8, pp. 3442–3452, 2017.
- [39] —, "Randomized turbo codes for the wiretap channel," in *IEEE Global Commun. Conf.*, 2017, pp. 1–6.
- [40] D. Kline, J. Ha, S. McLaughlin, J. Barros, and B. Kwak, "LDPC codes for the Gaussian wiretap channel," *IEEE Trans. Inf. Forensics and Security*, vol. 6, no. 3, pp. 532–540, 2011.

- [41] M. Baldi, M. Bianchi, and F. Chiaraluce, “Non-systematic codes for physical layer security,” in *IEEE Inf. Theory Workshop*, 2010, pp. 1–5.
- [42] M. Baldi, F. Chiaraluce, N. Laurenti, S. Tomasin, and F. Renna, “Secrecy transmission on parallel channels: Theoretical limits and performance of practical codes,” *IEEE Trans. Inf. Forensics and Security*, vol. 9, no. 11, pp. 1765–1779, 2014.
- [43] W. Harrison, E. Beard, S. Dye, E. Holmes, K. Nelson, M. Gomes, and J. Vilela, “Implications of coding layers on physical-layer security: A secrecy benefit approach,” *Entropy*, vol. 21, no. 8, p. 755, 2019.
- [44] C. Wong, T. Wong, and J. Shea, “LDPC code design for the BPSK-constrained Gaussian wiretap channel,” in *IEEE GLOBECOM Workshops*, 2011, pp. 898–902.
- [45] M. Baldi, G. Ricciutelli, N. Maturo, and F. Chiaraluce, “Performance assessment and design of finite length LDPC codes for the Gaussian wiretap channel,” in *IEEE Int. Conf. Commun. Workshop*, 2015, pp. 435–440.
- [46] A. Nooraiepour, S. Aghdam, and T. Duman, “On secure communications over Gaussian wiretap channels via finite-length codes,” *IEEE Commun. Letters*, vol. 24, no. 9, pp. 1904–1908, 2020.
- [47] T. O’Shea and J. Hoydis, “An introduction to deep learning for the physical layer,” *IEEE Trans. Cognitive Commun. Networking*, vol. 3, no. 4, pp. 563–575, 2017.
- [48] S. Dörner, S. Cammerer, J. Hoydis, and S. Brink, “Deep learning based communication over the air,” *IEEE J. Selected Topics Signal Processing*, vol. 12, no. 1, pp. 132–143, 2018.
- [49] F. Aoudia and J. Hoydis, “End-to-end learning of communications systems without a channel model,” in *Asilomar Conf. Signals, Systems, and Computers*, 2018, pp. 298–303.
- [50] M. Goutay, F. A. Aoudia, and J. Hoydis, “Deep reinforcement learning autoencoder with noisy feedback,” pp. 1–6, 2019.
- [51] R. Fritschek, R. Schaefer, and G. Wunder, “Deep learning for channel coding via neural mutual information estimation,” in *IEEE Int. Workshop Signal Processing Advances Wirel. Commun.*, 2019, pp. 1–5.
- [52] H. Ye, G. Li, F. Juang, and K. Sivanesan, “Channel agnostic end-to-end learning based communication systems with conditional GAN,” in *IEEE Globecom Workshops*, 2018, pp. 1–5.
- [53] R. Fritschek, R. Schaefer, and G. Wunder, “Deep learning for the Gaussian wiretap channel,” in *IEEE Int. Conf. Commun.*, 2019, pp. 1–6.
- [54] —, “Deep learning based wiretap coding via mutual information estimation,” in *ACM Workshop on Wireless Security and Machine Learning*, 2020, pp. 74–79.
- [55] K. Besser, P. Lin, C. Janda, and E. Jorswieck, “Wiretap code design by neural network autoencoders,” *IEEE Trans. Inf. Forensics and Security*, vol. 15, pp. 3374–3386, 2020.
- [56] D. P. Kingma and J. Ba, “Adam: A method for stochastic optimization,” *arXiv preprint arXiv:1412.6980*, 2014.
- [57] Y. Polyanskiy, H. Poor, and S. Verdu, “Channel coding rate in the finite blocklength regime,” *IEEE Trans. Inf. Theory*, vol. 56, no. 5, pp. 2307–2359, 2010.
- [58] R. F. Schaefer, H. Boche, and H. V. Poor, “Secure communication under channel uncertainty and adversarial attacks,” *Proceedings of the IEEE*, vol. 103, no. 10, pp. 1796–1813, 2015.
- [59] H. Boche, R. F. Schaefer, and H. V. Poor, “On the continuity of the secrecy capacity of compound and arbitrarily varying wiretap channels,” *IEEE Trans. Inf. Forensics and Security*, vol. 10, no. 12, pp. 2531–2546, 2015.
- [60] R. A. Chou and A. Yener, “The Gaussian multiple access wiretap channel when the eavesdropper can arbitrarily jam,” in *IEEE Int. Symp. Inf. Theory*, 2017, pp. 1958–1962.